Supporting Information

Investigation on local structures of Si-Cr-based solvents via ab initio molecular dynamics

Guangda Chen[a], Zhongnan Guo[a,*], Wenlong Wu[a], Zihai Li[a], Peirou Ji[a], Lishi Chen[a], Yunfan Yang[b], Da Sheng[b], Hui Li[b], Wenxia Yuan[a,*]

[a]*Department of Chemistry, School of Chemistry and Biological Engineering, University of Science and Technology Beijing, Beijing, 100083, PR China*

[b]*Beijing National Laboratory for Condensed Matter Physics, Institute of Physics, Chinese Academy of Sciences, Beijing, 100190, China*

E-mail: guozhongn@ustb.edu.cn (Z. Guo), wxyuanwz@163.com (W. Yuan)

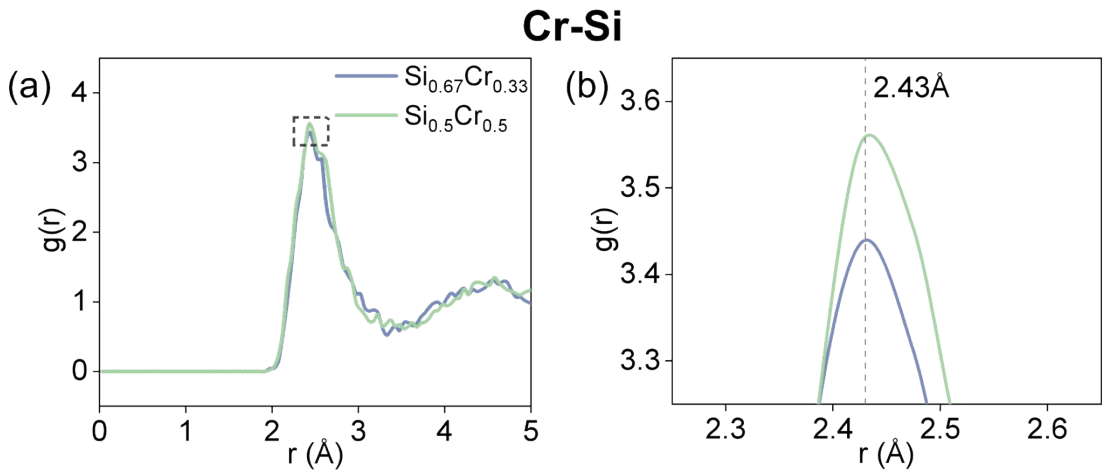

Fig. S1. (a) The $g_{Cr\text{-}Si}(r)$ curves in $Si_{0.67}Cr_{0.33}$ and $Si_{0.5}Cr_{0.5}$ melts. (b) Enlarged view of the dashed box region in (a).

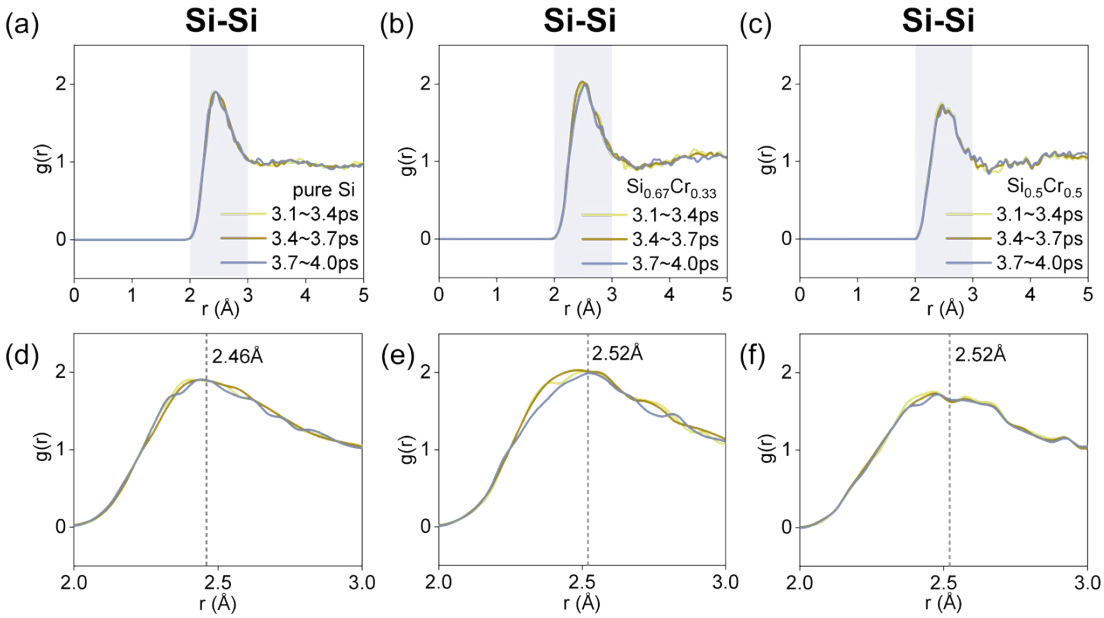

Fig. S2. For (a) pure Si, (b) $Si_{0.67}Cr_{0.33}$, and (c) $Si_{0.5}Cr_{0.5}$ melts, the $g_{S\text{-}Si}(r)$ curves were statistically analyzed within the simulation time ranges of 3.1–3.4 ps, 3.4–3.7 ps, and 3.7–4.0 ps, respectively, to verify the statistical stability of Si-Si interaction characteristics. (d), (e), and (f) show local enlargements of the first peak of the $g_{S\text{-}Si}(r)$ curves in (a), (b) and (c), respectively.

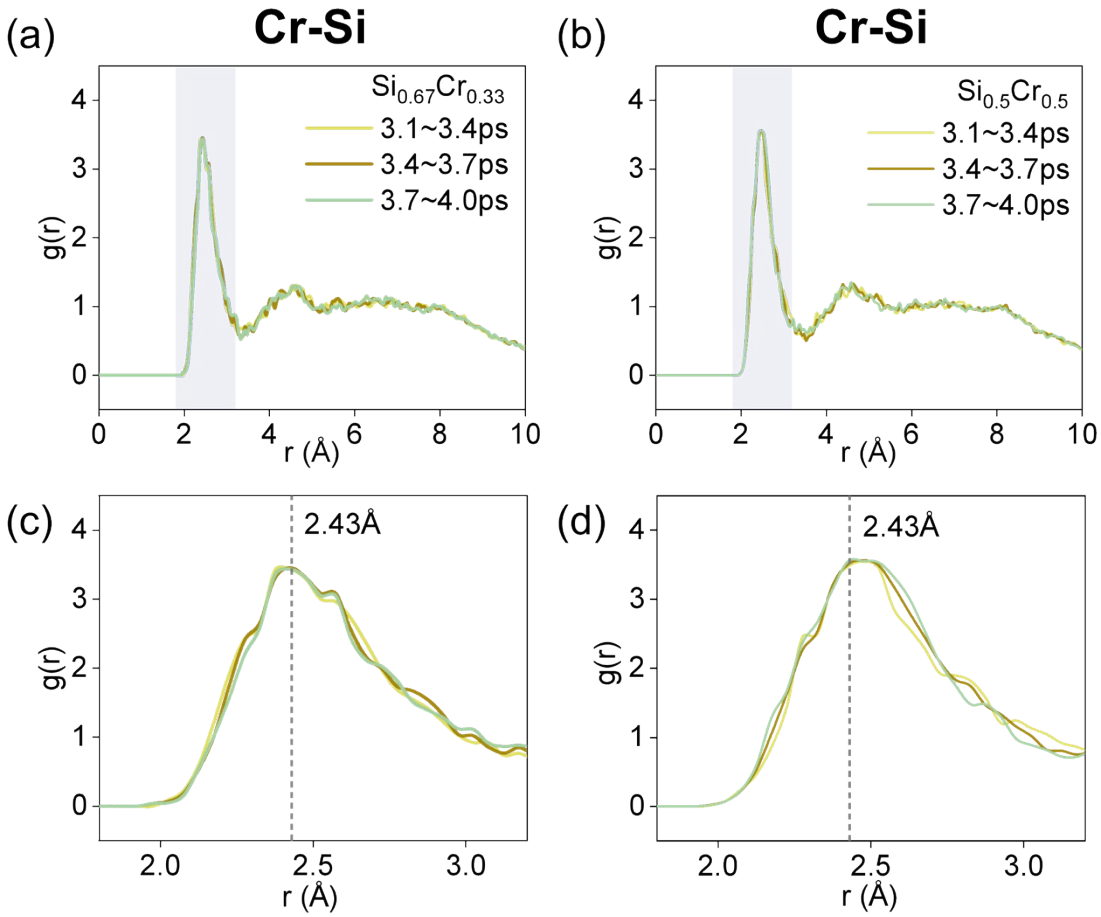

Fig. S3. For (a) $Si_{0.67}Cr_{0.33}$ and (b) $Si_{0.5}Cr_{0.5}$ melts, the $g_{Cr\text{-}Si}(r)$ curves were statistically analyzed within the simulation time ranges of 3.1–3.4 ps, 3.4–3.7 ps, and 3.7–4.0 ps, respectively, to verify the statistical stability of Si-Si interaction characteristics. (c) and (d) show local enlargements of the first peak of the $g_{Cr\text{-}Si}(r)$ curve in (a) and (b), respectively.

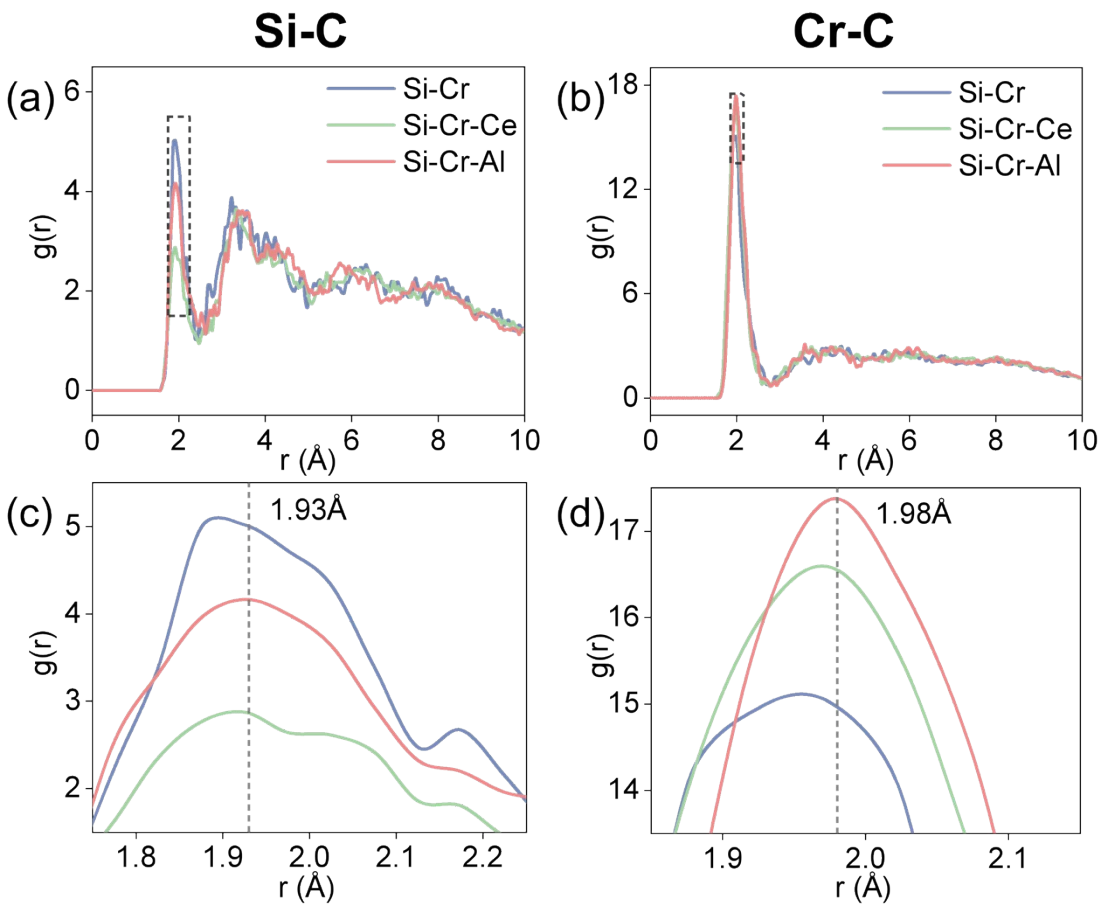

Fig. S4. The (a) $g_{Si\text{-}C}(r)$ and (b) $g_{Cr\text{-}C}(r)$ in Si-Cr, Si-Cr-Ce and Si-Cr-Al solvents in contact with 4H-C. (c) and (d) are enlarged view of the dashed box region in (a) and (b), respectively.

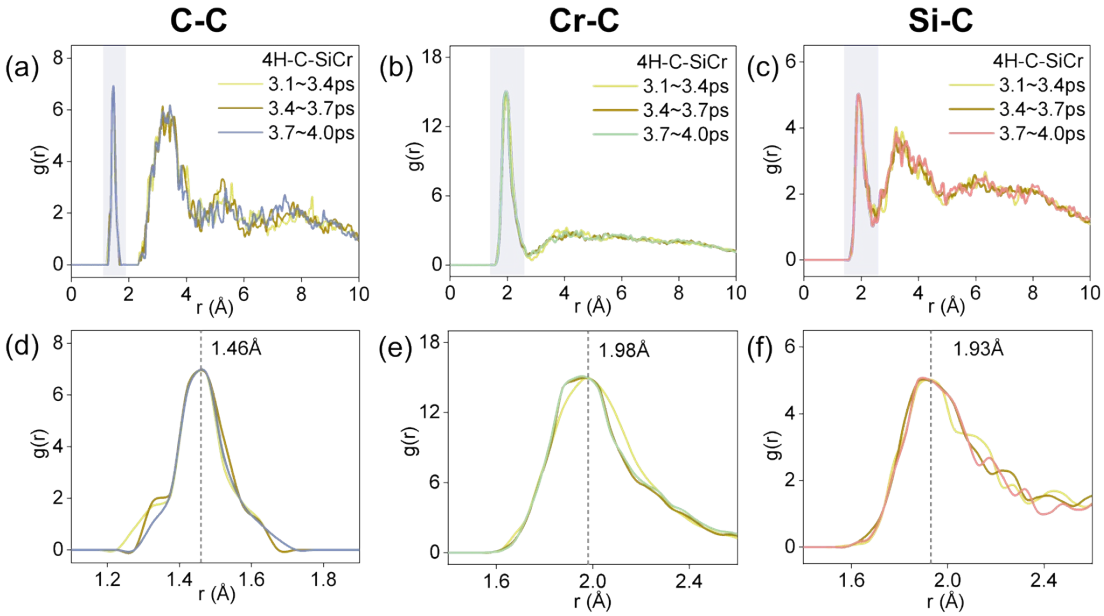

Fig. S5. The (a) $g_{C\text{-}C}(r)$, (b) $g_{Cr\text{-}C}(r)$ and (c) $g_{Si\text{-}C}(r)$ curves of Si-Cr solvent in contact with 4H-C were statistically analyzed within the simulation time ranges of 3.1–3.4 ps, 3.4–3.7 ps, and 3.7–4.0 ps, respectively, to verify the statistical stability. (d), (e), and (f) show local enlargements of the first peak of g(r) curves in (a), (b) and (c), respectively.

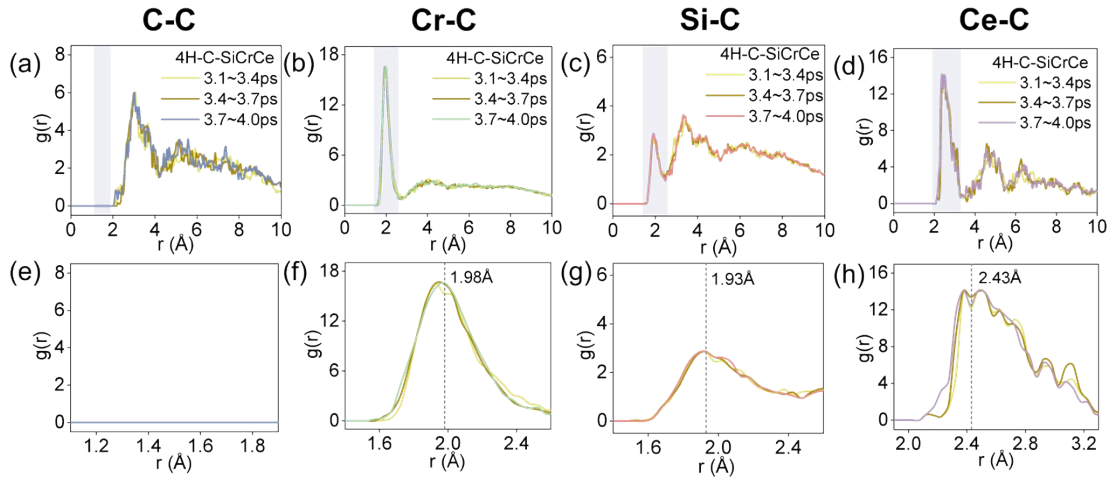

Fig. S6. The (a) $g_{C\text{-}C}(r)$, (b) $g_{Cr\text{-}C}(r)$, (c) $g_{Si\text{-}C}(r)$ and (d) $g_{Ce\text{-}C}(r)$ curves of Si-Cr-Ce solvent in contact with 4H-C were statistically analyzed within the simulation time ranges of 3.1–3.4 ps, 3.4–3.7 ps, and 3.7–4.0 ps, respectively, to verify the statistical stability. (e), (f), (g) and (h) show local enlargements of the first peak of g(r) curves in (a), (b), (c) and (d) respectively.

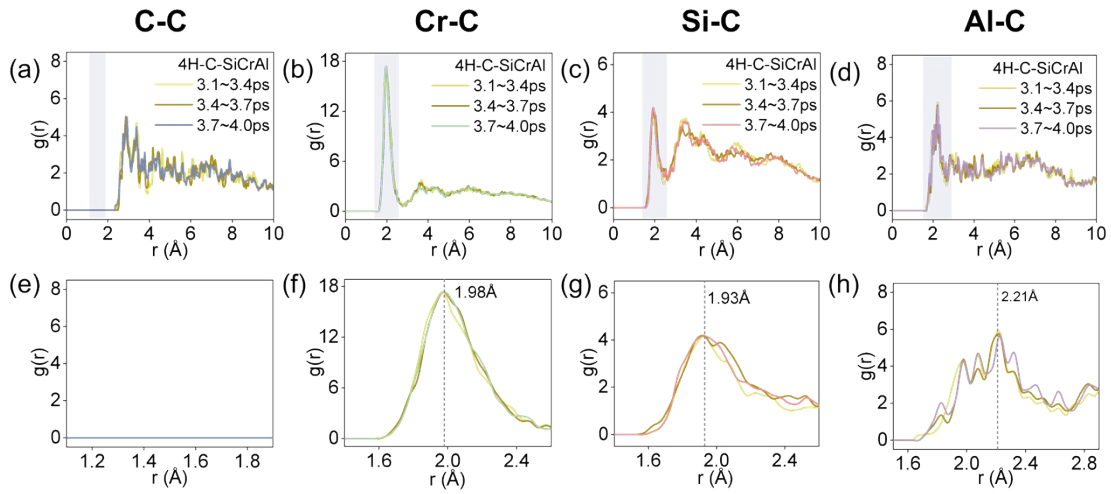

Fig. S7. The (a) $g_{C\text{-}C}(r)$, (b) $g_{Cr\text{-}C}(r)$, (c) $g_{Si\text{-}C}(r)$ and (d) $g_{Al\text{-}C}(r)$ curves of Si-Cr-Al solvent in contact with 4H-C were statistically analyzed within the simulation time ranges of 3.1–3.4 ps, 3.4–3.7 ps, and 3.7–4.0 ps, respectively, to verify the statistical stability. (e), (f), (g) and (h) show local enlargements of the first peak of g(r) curves in (a), (b), (c) and (d) respectively.

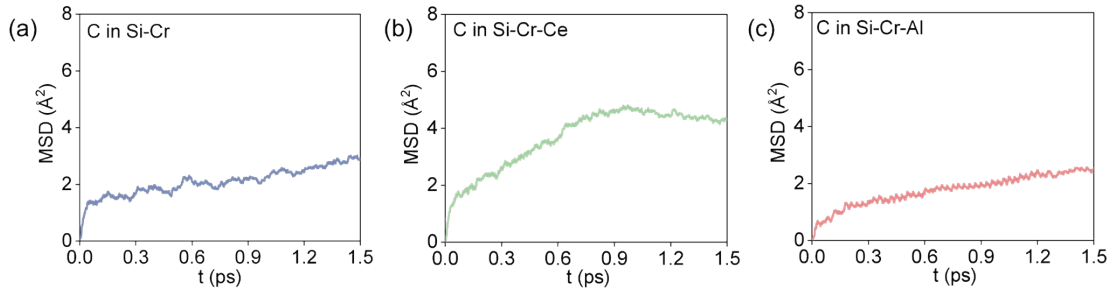

Fig. S8. The MSD curves of C atoms in (a) Si-Cr, (b) Si-Cr-Ce and (c) Si-Cr-Al solvents in contact with the 4H-C face.

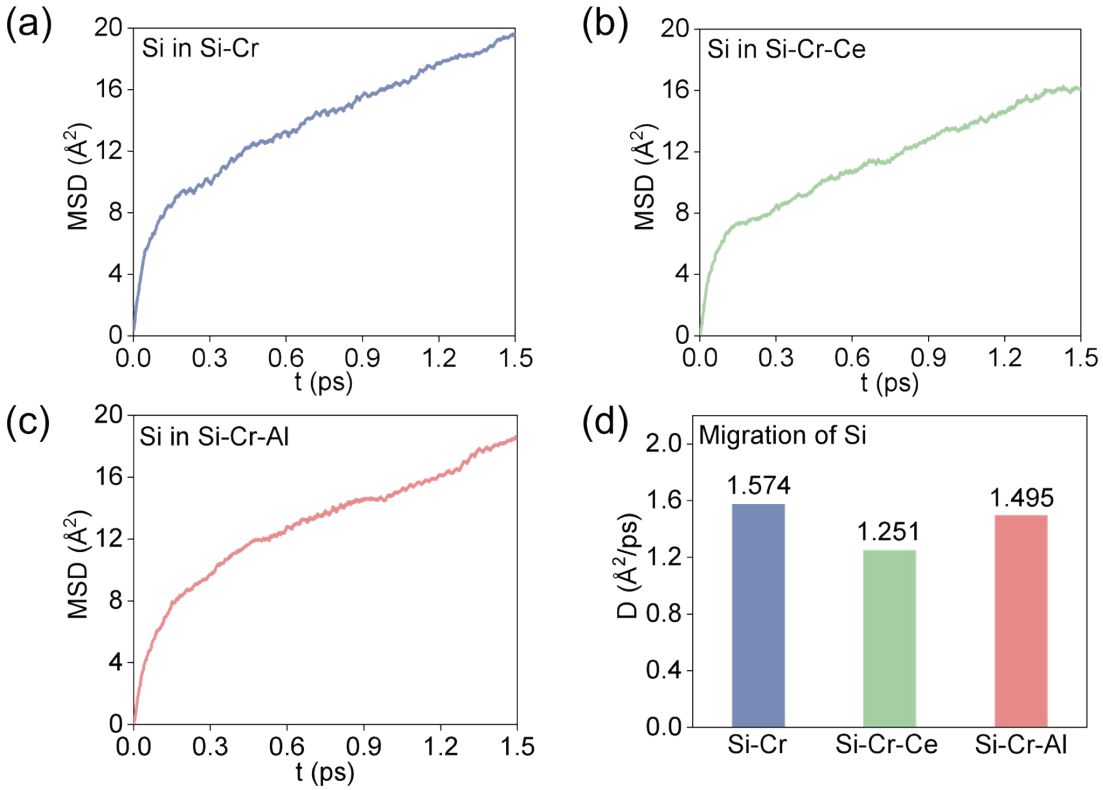

Fig. S9. The MSD curves of Si atoms in (a) Si-Cr, (b) Si-Cr-Ce and (c) Si-Cr-Al solvents in contact with the 4H-C face. (d) Diffusion coefficient of Si in the three solvents.

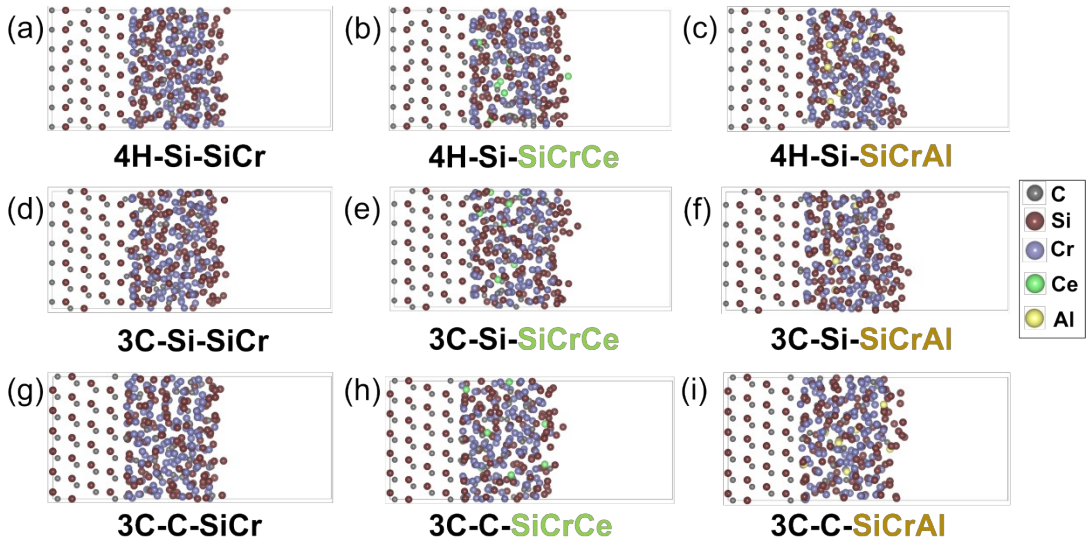

Fig. S10. The supercell configurations of (a) Si-Cr, (b) Si-Cr-Ce (c) Si-Cr-Al solvents in contact with 4H-Si. The supercell configuration of (d) Si-Cr, (e) Si-Cr-Ce, (f) Si-Cr-Al solvents in contact with 3C-Si. The supercell configuration of (g) Si-Cr, (h) Si-Cr-Ce, (i) Si-Cr-Al solvents in contact with 3C-C.

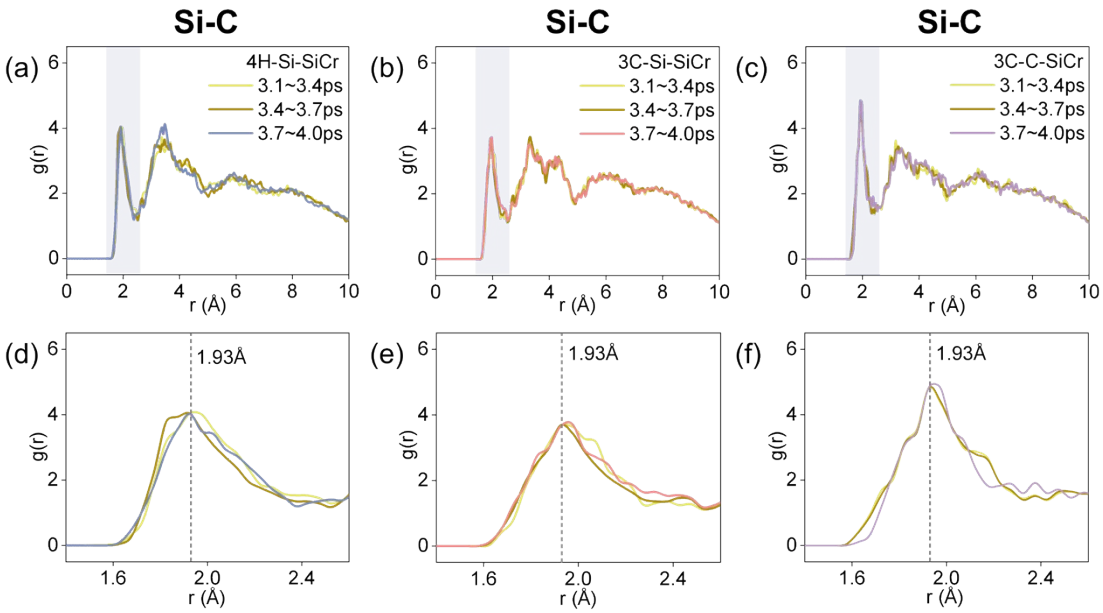

Fig. S11. The $g_{Si\text{-}C}(r)$ curves of Si-Cr solvents in contact with (a) 4H-Si, (b) 3C-Si and (c) 3C-C were statistically analyzed within the simulation time ranges of 3.1–3.4 ps, 3.4–3.7 ps, and 3.7–4.0 ps, respectively, to verify the statistical stability. (d), (e) and (f) show local enlargements of the first peak of g(r) curves in (a), (b) and (c), respectively.

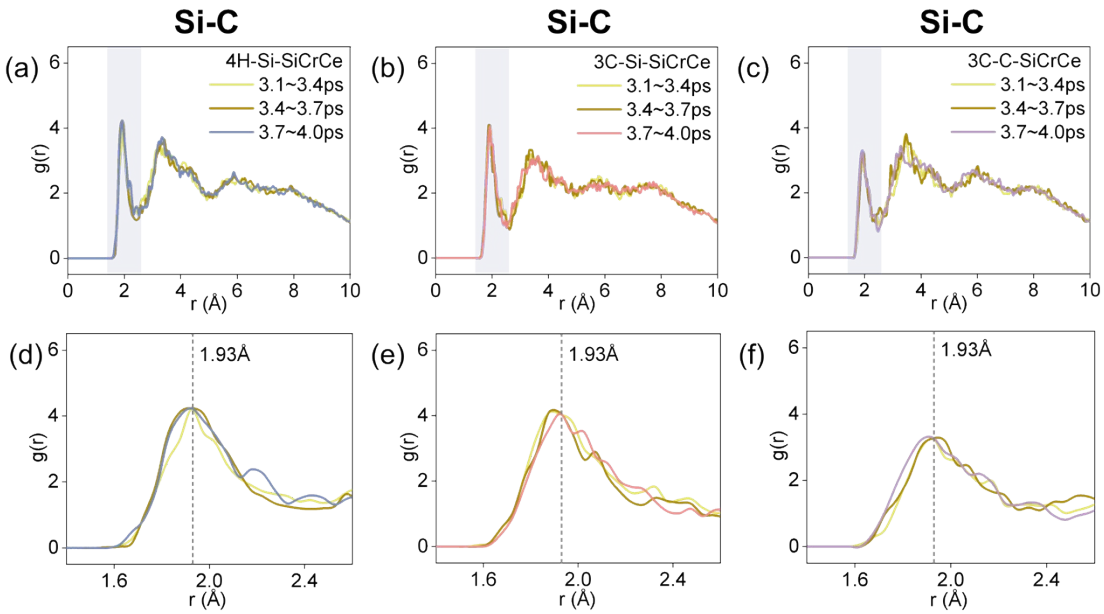

Fig. S12. The $g_{Si\text{-}C}(r)$ curves of Si-Cr-Ce solvents in contact with (a) 4H-Si, (b) 3C-Si and (c) 3C-C were statistically analyzed within the simulation time ranges of 3.1–3.4 ps, 3.4–3.7 ps, and 3.7–4.0 ps, respectively, to verify the statistical stability. (d), (e) and (f) show local enlargements of the first peak of g(r) curves in (a), (b) and (c), respectively.

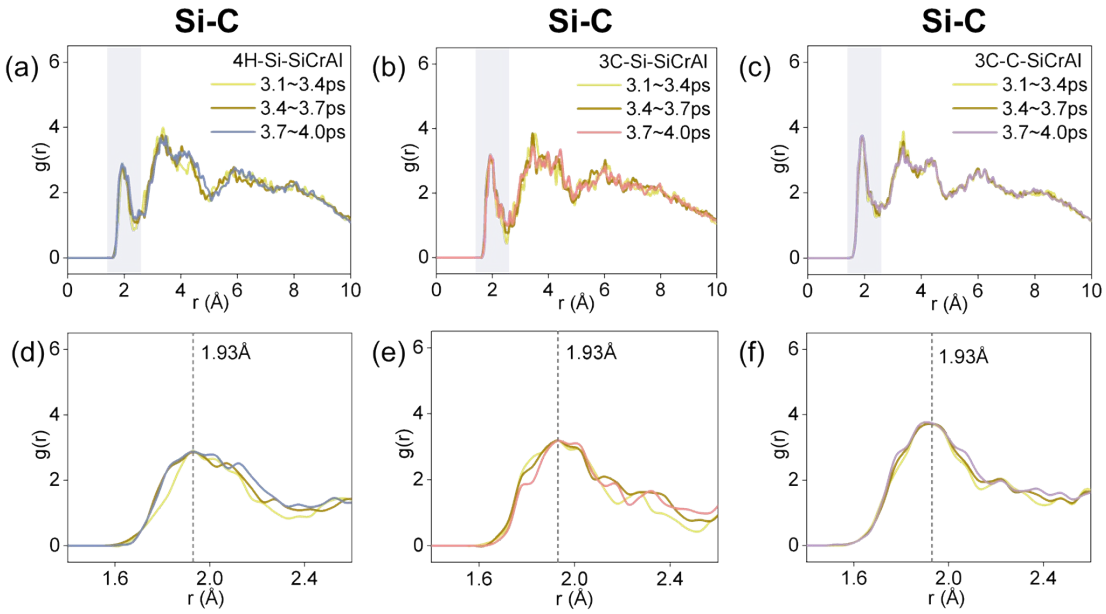

Fig. S13. The $g_{Si\text{-}C}(r)$ curves of Si-Cr-Al solvents in contact with (a) 4H-Si, (b) 3C-Si and (c) 3C-C were statistically analyzed within the simulation time ranges of 3.1–3.4 ps, 3.4–3.7 ps, and 3.7–4.0 ps, respectively, to verify the statistical stability. (d), (e) and (f) show local enlargements of the first peak of g(r) curves in (a), (b) and (c), respectively.

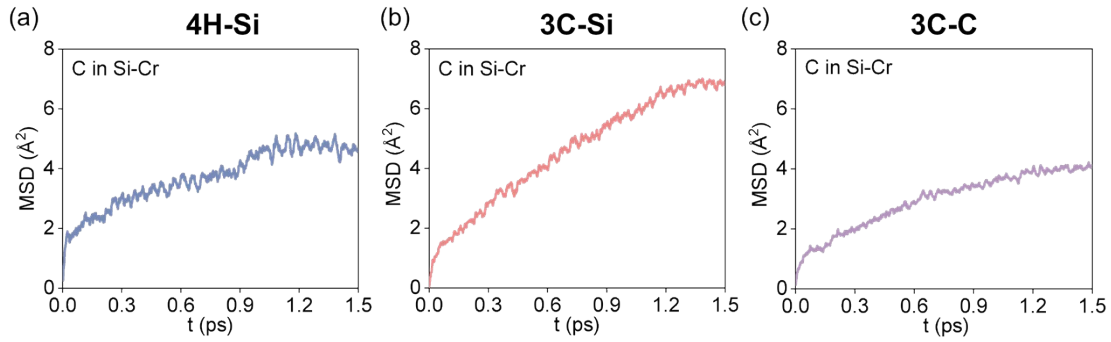

Fig. S14. The MSD curves of C atoms in Si-Cr solvents in contact with (a) 4H-Si, (b) 3C-Si and (c) 3C-C.

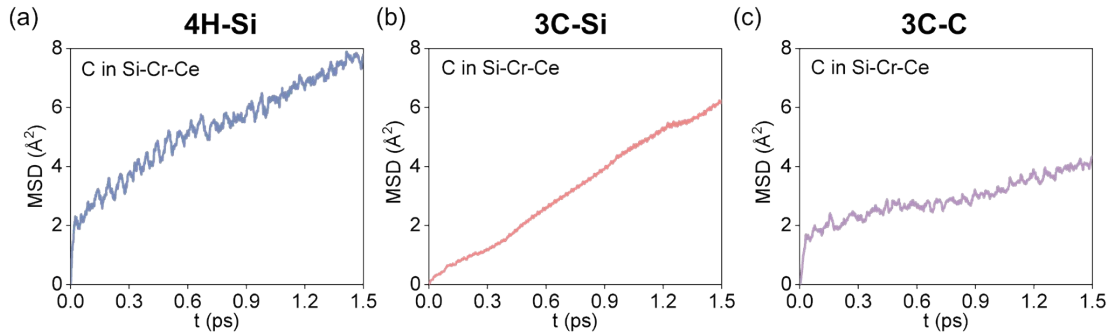

Fig. S15. The MSD curves of C atoms in Si-Cr-Ce solvents in contact with (a) 4H-Si, (b) 3C-Si and (c) 3C-C.

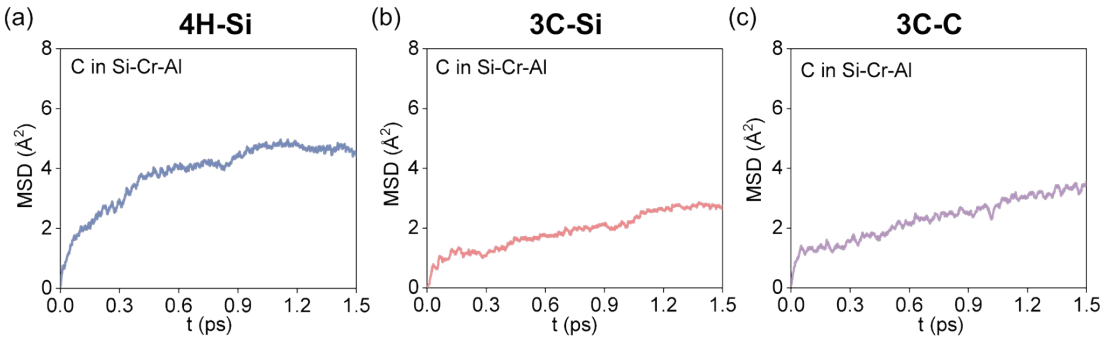

Fig. S16. The MSD curves of C atoms in Si-Cr-Al solvents in contact with (a) 4H-Si, (b) 3C-Si and (c) 3C-C.

Table S1. The calculated diffusion coefficients of C atoms in different models within different simulation durations.

Models	Diffusion coefficients of C ($Å^2$/ps)		
	0~3ps	0~3.5ps	0~4ps
4H-Si/Si-Cr	0.372	0.373	0.375
4H-C/Si-Cr	0.152	0.165	0.161
3C-Si/Si-Cr	0.673	0.657	0.647
3C-C/Si-Cr	0.382	0.367	0.360
4H-Si/Si-Cr-Ce	0.548	0.529	0.531
4H-C/Si-Cr-Ce	0.454	0.412	0.432
3C-Si/Si-Cr-Ce	0.703	0.725	0.729
3C-C/Si-Cr-Ce	0.247	0.270	0.266
4H-Si/Si-Cr-Al	0.390	0.380	0.355
4H-C/Si-Cr-Al	0.199	0.183	0.185
3C-Si/Si-Cr-Al	0.240	0.252	0.245
3C-C/Si-Cr-Al	0.267	0.251	0.263

Table S2. The calculated diffusion coefficients of Ce atoms in different models within different simulation durations.

Solid/Liquid interface	Diffusion coefficients of Ce ($Å^2$/ps)		
	0~3ps	0~3.5ps	0~4ps
4H-Si/Si-Cr-Ce	0.339	0.319	0.313
4H-C/Si-Cr-Ce	1.56	1.62	1.58
3C-Si/Si-Cr-Ce	6.98	6.83	6.88
3C-C/Si-Cr-Ce	2.75	2.65	2.65